Publishing House
AKAPIT

COMPUTER METHODS IN MATERIALS SCIENCE
Informatyka w Technologii Materiałów

Vol. 14, 2014, No. 2

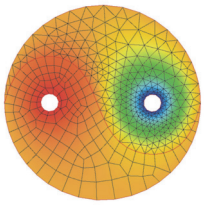

MATHEMATICAL MODELLING OF THE TUNDISH INERTIZATION PRACTICE

BERNARDO MARTINS BRAGA, ROBERTO PARREIRAS TAVARES*

Metallurgical and Materials Engineering Department, Engineering School,
Federal University of Minas Gerais
Ave. Presidente Antônio Carlos 6627, 31270-901 Belo Horizonte, Brazil
**Corresponding author: rtavares@demet.ufmg.br*

Abstract

The inertization practice for a 17.7 tons of steel continuous casting tundish has been studied by means of a three-dimensional non-isothermal mathematical model. The model considers a single gaseous phase composed of argon and air. Turbulence was accounted for with the standard k-ε model. The calculations were carried out using the commercial CFD software ANSYS CFX. Different configurations of the inertization system were simulated and a novel approach was utilized to discuss model findings. The results indicated that the present configuration is ineffective and new ones were suggested.

Key words: Tundish inertization, mathematical simulation, continuous casting, non-metallic inclusion

1. INTRODUCTION

The practice of tundish inertization (or purging) consists of the creation of an inert atmosphere inside this reactor before the first heat of a sequence. This technique is widely used to avoid productivity and yield losses arising from the contact between steel and air in the transient stages of the continuous casting process: initial filling of the tundish and ladle changes. If this contact occurs, oxygen present in the air reacts with liquid steel generating non-metallic inclusions and reducing the yield of alloy additions. Nitrogen also dissolves in the liquid steel increasing its content (Zhang & Thomas, 2003).

The interaction between liquid steel and air may also lead to downgrading or scraping of the steel, especially for high-grade steels that require high cleanliness and strict control of its chemical composition (Bonilla, 1995; Hughes et al., 1995; Chen et al., 2005; Yuan, 2009; Buoro & Romanelli, 2012). It also favors deposition of non metallic inclusions on the submerged entry nozzle, which connects the tundish to the mould, provoking its clogging (Riley, 1996; Mattedi et al., 2003).

Despite the importance of tundish inertization, there are few studies on the subject available in the open literature. Previous works are often based on industrial improvements and omit relevant information like the configuration of the injectors, lid design, tundish volume and inert gas flow rate. It is evident the massive implementation of in-house solutions that are treated as confidential information.

Based on contact with professionals from steel plants and on the literature review, inadequate inertization practices, carried out without appropriate design, dimensioning and efficiency analysis, were observed. These practices stem from the lack of information on the subject.

The design of inertization systems is usually based on the theory of completely mixed vessels. The efficiency analysis is performed mainly by experimental approach, such as trials on physical mod-

 ISSN 1641-8581

els and cold or hot industrial tests (Uesugi, 1985; Bannenberg & Harste, 1993; Riley, 1996; Chen et al., 2005). Mattedi et al. (2003) used a mathematical model, validated with industrial measurements, to design the inertization system for the former CST steelplant (now ArcelorMittal Tubarão). However, the authors provided few details about the inertization solution developed.

Riley (1996) developed important conceptual work on the topic. The author considers that the loss of efficiency in inertization systems occurs due to air entry arising from natural convection and turbulent jet entrainment. It was found empirically that the two mechanisms are approximately additive. The natural convection is attenuated by high flow rates and by lid openings closure. In turn, turbulent jet entrainment is reduced by low flow rates and by increasing the number and diameter of the injectors.

In the present work, a mathematical model was developed and used to investigate the tundish inertization process for a four strand continuous casting tundish. Purging was carried out by the injection of argon through pipes located at the tundish lid. The results of the simulations enabled the identification of more convenient practices for interization. A new approach was also proposed to discuss model results.

2.1. Mathematical Model

The mathematical model developed consists of the conservation equations of mass, momentum and energy (low Mach number formulation) for the gaseous mixture. It also includes the mass conservation equations for air and argon in terms of their mass fractions. Turbulence was modeled by means of the standard k-ε model with source terms related to production and non-directional dissipation of turbulence due to buoyancy (Ansys, 2012). Commercial software ANSYS CFX was used in the solution of the system of partial differential equations.

In the model, air and argon were treated as ideal gases. The heat capacity, thermal conductivity and viscosity of the air were collected from Incropera et al. (2006). All argon properties can be predicted theoretically. The values of thermal conductivity and viscosity, calculated by Bich et al. (1990) with relativistic corrections and the heat capacity of monatomic ideal gas (Atkins & De Paula, 2006), were adopted in all the calculations.

The air-argon diffusivity, mixture thermal conductivity and mixture viscosity were evaluated according to Bird et al. (2002). Temperature dependence of all materials properties were estimated by algebraic expressions or using an inversion table scheme.

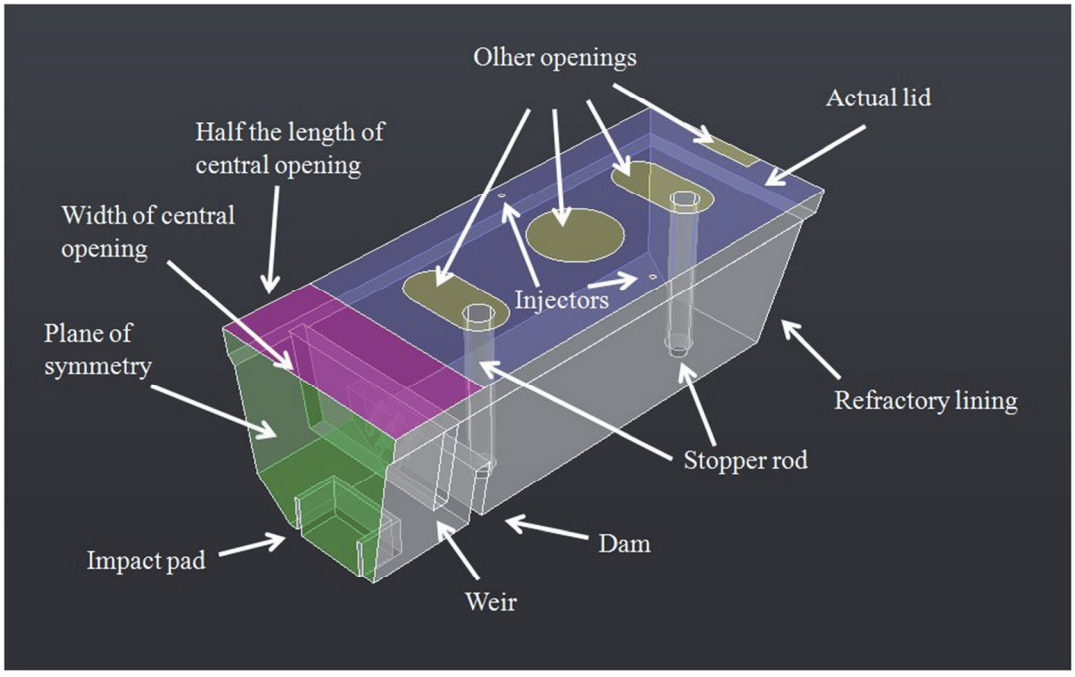

Fig. 1. *Schematic view of the tundish with argon injection by four 25.4mm pipes in the lid (configurations C1, C4 and H1, see tables 1 and 2). Due to symmetry, only one half of the domain was simulated.*

2. METHODOLOGY

Figure 1 shows a schematic view of the tundish considered in the present study. Due to system symmetry, only one half of domain was simulated.

In order to analyze separately the two air entrainment mechanisms and to obtain more general results, tundish inertization configurations considering cold and hot starts were simulated. The conditions adopted in the simulations are presented in tables 1 and 2. In the former case, initial air temperature inside the tundish and tundish refractory temperature were assumed to be 25°C. In the latter case, a temperature of 1200°C was assigned. In the present work, 1Nm³ stands for 1m³ of gas measured at 1atm (101325Pa) and 0°C (273.15K).

Main features of the tundish, boundary conditions used and the initial condition imposed on the model are shown in tables 3, 4 and 5, respectively. Ambient pressure of 1atm was assumed in all the calculations.

Figure 2 shows the injectors distribution in the tundish lid considered in the present work.

The mathematical model predicts the evolution of the argon molar fraction and temperature at each point of the tundish and their average values.

In the configurations considering cold start, 5 minutes of purging were simulated. This is the maximum time available for purging in the industry. Considering hot start, the argon content stabilizes more rapidly and only 2.5 minutes were simulated.

Table 1. *Configurations analyzed in the inertization of the tundish considering cold start.*

Configurations	C1	C2	C3	C4	C5	C6	C7
Flow rate (Nm³/h)	70	70	70	560	70	105	140
No. of injectors	4	12	4	4	4	4	4
Injector diameter (mm)	25.4	25.4	76.2	25.4	25.4	25.4	25.4
Width of central opening (mm)	1038.2	1038.2	1038.2	1038.2	920.7	920.7	920.7
Length of central opening (mm)	920	920	920	920	596	596	596
Other openings	Opened	Opened	Opened	Opened	Closed	Closed	Closed

Table 2. *Configurations analyzed in the inertization of the tundish considering hot start.*

Configurations	H1	H2	H3	H4
Flow rate (Nm³/h)	70	70	105	140
No. of injectors	4	4	4	4
Injector diameter (mm)	25.4	25.4	25.4	25.4
Width of central opening (mm)	1038.2	920.7	920.7	920.7
Length of central opening (mm)	920	596	596	596
Other openings	Opened	Closed	Closed	Closed

Table 3. *Main features of tundish.*

Nominal capacity (tons)	17.7	Opened area on the lid (m²), configurations C1 to C4 and H1	1.70
Internal volume (m³)	3.20	Opened area on the lid (m²), configurations C5 to C7 and H2 to H4	0.55

Table 4. *Boundary conditions used in the mathematical model.*

Inlet		Openings*		Refractories and lid
Profile	Uniform	Relative pressure (Pa)	0	Constant temperature
Gas distribution among injectors	Uniform	Direction	Normal	No-slip condition
Temperature (ºC)	25	Temperature (ºC)	25	Hydraulically smooth wall
Turbulence intensity** (%)	5	Turbulence intensity** (%)	1	Scalable wall function
Eddy viscosity ratio***	10	Eddy viscosity ratio***	1	Symmetry
Air mass fraction	0	Air mass fraction	1	Zero-flux
* Total relative pressure is used for gas inlet and static pressure for gas outlet. Other parameters are used only if there is air entrainment (Ansys, 2012).				
** Relation (I) between the fluctuating component of fluid velocity (u), existing in turbulent flows, and the average fluid velocity (U): I = u / U (Ansys, 2012).				
*** Ratio (R) between the turbulent viscosity (μ_t), introduced by Boussinesq hypothesis, and the dynamic viscosity of material (μ): R = μ_t / μ (Ansys, 2012).				

Table 5. *Initial conditions imposed on the mathematical model.*

Velocity within the domain	Null	Turbulence intensity (%)	1
Pressure within the domain	Hydrostatic	Eddy viscosity ratio	1
Temperature within the domain	Uniform	Air mass fraction	1

ously and therefore promotes additional air entry. Natural convection is created by resultant force R_b (N) that arises from the inhomogeneity of the temperature field within the tundish. The parameter R_b can be estimated from buoyancy and weight forces:

$$R_b = \int_{V_t} g(\rho_{air} - \rho)dV = g(\rho_{air} - \bar{\rho})V_t \quad (2)$$

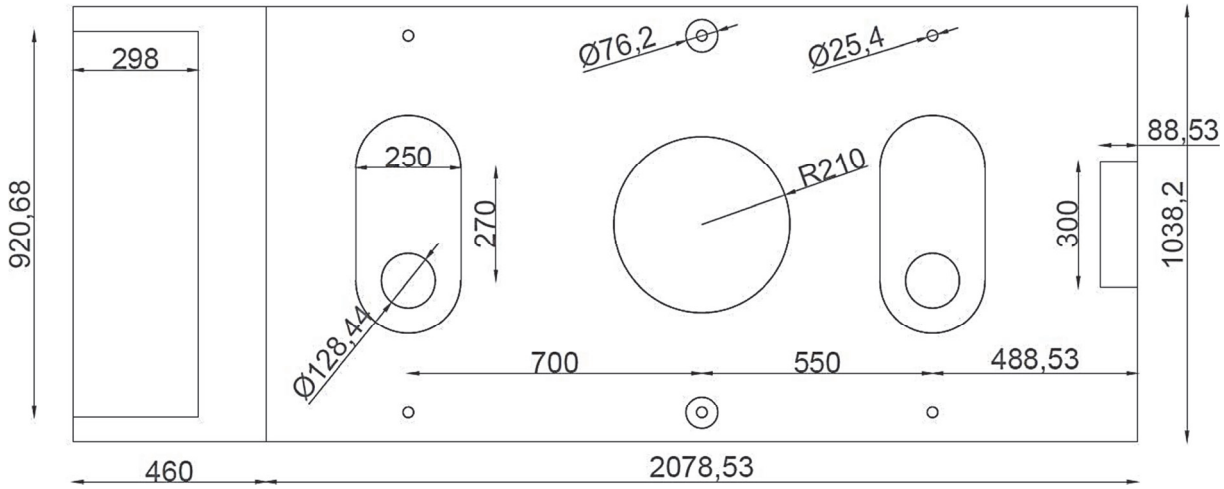

Fig. 2. *Schematic view of the tundish lid used in this work with all configurations of the central opening and injectors superimposed. In the configurations that use 4 injectors, just the central pipes are modeled. All dimensions are in millimeters.*

For ensuring the numerical accuracy of the model, studies of mesh and time-step independence were carried out. Final simulations adopted tetrahedral meshes of approximately 330 thousand elements (80 thousand nodes) and time-step of 0.1s.

2.2. Approach to Discuss Inertization Efficiency

During purging of a tundish with cold start, the driving force for fluid flow and hence air entry is J_{in} (N), the *momentum* input rate of the injected gas. So one logical way of improving inertization efficiency is to control J_{in} magnitude and its distribution within the tundish. The parameter J_{in} can be calculated as follows:

$$J_{in} = \int_{A_{in}} \rho_{in} {w_{in}}^2 dA = \frac{{\dot{m}_{in}}^2}{\rho_{in} A_{in}} = \frac{4}{\pi}\frac{1}{\rho_{in}}\frac{{\dot{m}_{in}}^2}{nd^2} \quad (1)$$

Where ρ_{in} is the argon density (kg/m³) measured at inlet conditions, w_{in} is the inlet velocity (m/s), A_{in} is the total area of injectors (m²), dA is a infinitesimal element of area (m²), $\dot{m}_{in}$ $(= \rho_{in} w_{in} A_{in})$ is the injected mass flow rate (kg/s), n is the number of injectors and d the diameter of injectors (m).

During inertization of a tundish with hot start, another driving force for fluid flow acts simultane-

Where g is the acceleration due to gravity (m/s²), ρ_{air} is the air density (kg/m³) measured at ambient conditions, ρ is the mixture density (kg/m³) measured at local conditions, V_t is the internal volume (m³) of the tundish, dV is a infinitesimal element of volume (m³) and $\bar{\rho}$ is the average density (kg/m³) of the fluid present within the tundish:

$$\bar{\rho} = \frac{1}{V_t}\int_{V_t} \rho \, dV \approx \frac{p_{amb}}{RT}(N_{Ar}M_{Ar} + N_{air}M_{air}) \quad (3)$$

Where p_{amb} is the ambient pressure (Pa), R is the universal gas constant (J/mol K), T is the average tundish temperature (K), N_{Ar} is the average argon molar fraction, M_{Ar} is the argon molar mass (kg/mol), N_{air} is the average air molar fraction $(= 1 - N_{Ar})$ and M_{air} is the air molar mass (kg/mol).

According to data provided by Bird et al. (2002), M_{Ar} (39.948g/mol) does not differ greatly from M_{air} (28.964g/mol). So the resultant force R_b is essentially a function of the average tundish temperature T wherein R_b increases with augmentation of T.

In tundishes with both cold start and hot start, the tendency of air entry is counterbalanced by the *momentum* output rate of the exiting gas that acts in outward direction on lid openings preventing air entrainment. But to improve purging efficiency, it is

interesting to increase just the part related to argon J_{out} (N), since the part related to air will inherently lead to some air entry. The parameter J_{out} can be roughly approximated as:

$$J_{out} = \int_{A_{out}} \rho_{Ar} {w_{Ar}}^2 dA \approx \frac{{\dot{m}_{in}}^2}{\rho_t A_{out}} \qquad (4)$$

Where ρ_{Ar} is the argon density (kg/m³) measured at local conditions, ρ_t is the argon density (kg/m³) measured at p_{amb} and T, w_{Ar} is the argon velocity-component normal to lid openings (m/s) and A_{out} is the lid openings area (m²).

3. RESULTS AND DISCUSSION

3.1. Inertization of Tundish Considering Cold Start

Figure 3 shows the time variation of the average argon molar fraction (N_{Ar}) during purging for configurations of tundish inertization considering cold start. Table 6 summarizes N_{Ar} values at the end of purging predicted by the mathematical model for the same configurations. Figure 4 shows contour plots for the normal velocity component at the lid opening at the end of purging for the previous configurations. Negative values indicate flow in inward direction and therefore point out air entry.

Configuration C1 corresponds to cold start version of the present configuration used in the plant (H1). The predicted argon molar fraction (N_{Ar} = 0.72) indicates a moderate purging efficiency. A complete inertization of the tundish was hindered by air entry that takes place through the lid openings near the injectors, as can be seen in figure 4a.

Table 6. *Average argon molar fraction (N_{Ar}) inside the tundish at the end of purging predicted by the mathematical model for configurations of tundish inertization considering cold start.*

Configuration	N_{Ar}
C1	0.72
C2	0.85
C3	0.90
C4	0.33
C5	0.89
C6	0.97
C7	0.99

In configuration C2, the number of injectors was tripled in relation to configuration C1 (4 to 12), thus J_{in} was reduced to one third. The *momentum* source was also homogenized. As a result, air entry was reduced (figure 4b) and purging efficiency was improved (N_{Ar} = 0.85). On the other hand, in configuration C3, the diameter of injectors was tripled in relation to configuration C1 (25.4mm to 76.2mm), so J_{in} was reduced to one ninth of its initial value. As a result, air entry was suppressed (figure 4c) and purging efficiency was further improved (N_{Ar} = 0.90).

The attempt to enhance purging efficiency of configuration C1 by exaggerated increase of argon flow rate (70Nm³/h to 560Nm³/h) corresponds to configuration C4. It is noted that argon molar fraction drops significantly (N_{Ar} = 0.33). Gas flow rate was increased eightfold, hence J_{in} was raised 64 times. As a result, air entry was worsened and occurs even at the central opening (figure 4d). This result

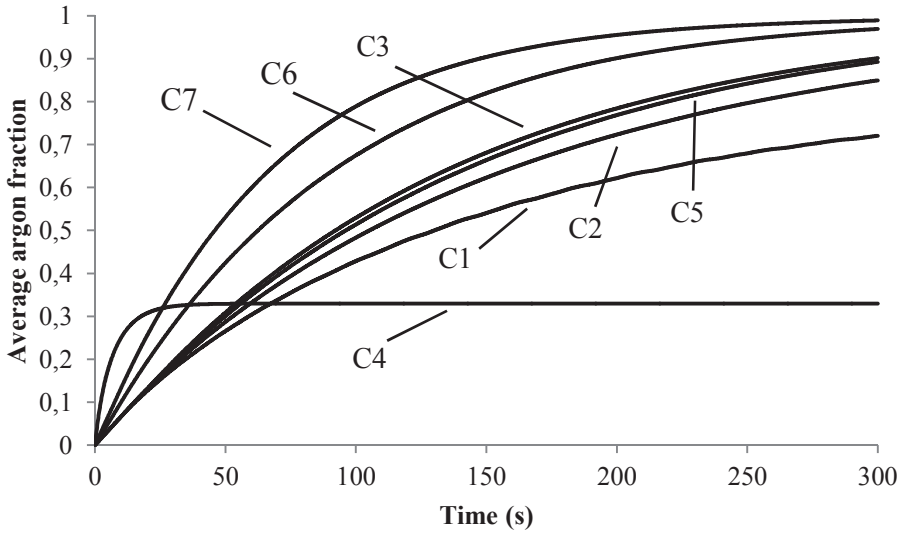

Fig. 3. *Time variation of average argon molar fraction (N_{Ar}) during purging for configurations of tundish inertization considering cold start. Values represent volumetric averages within the tundish.*

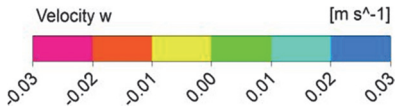

a)

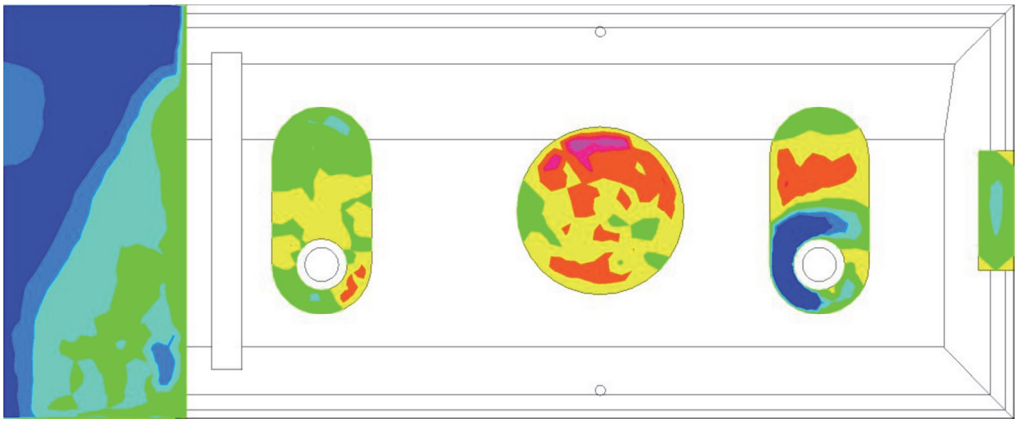

b)

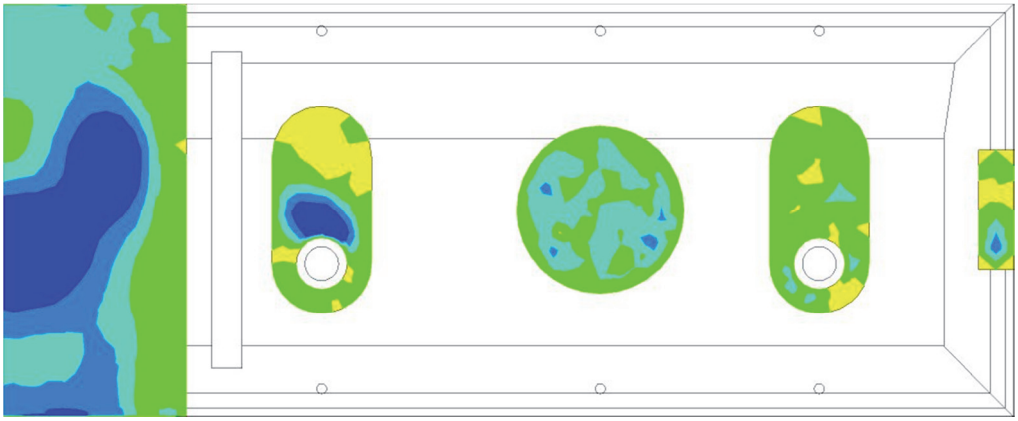

c)

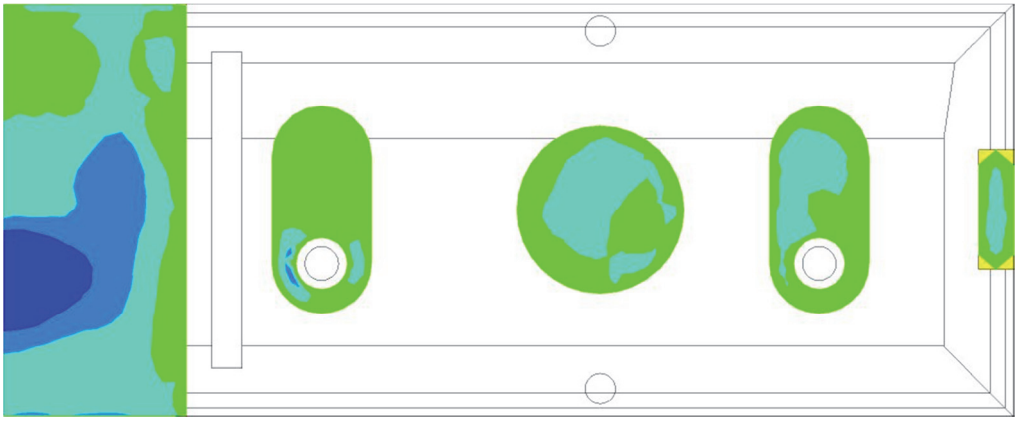

d)

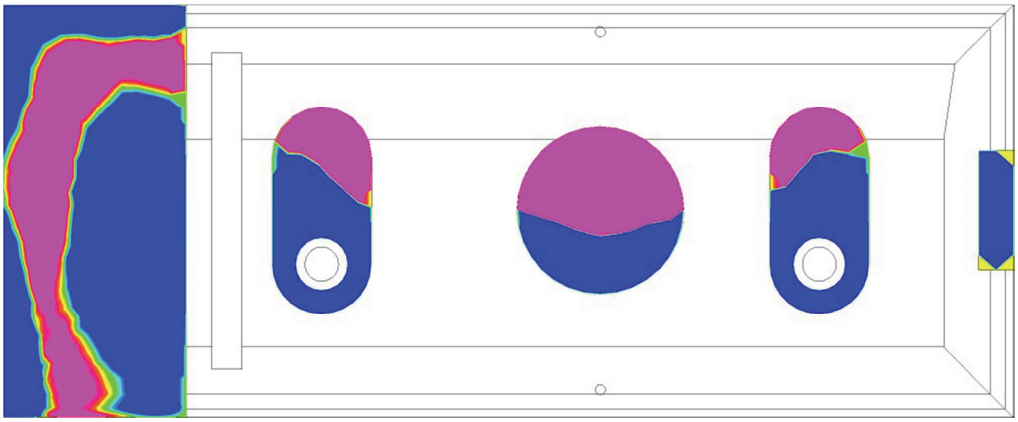

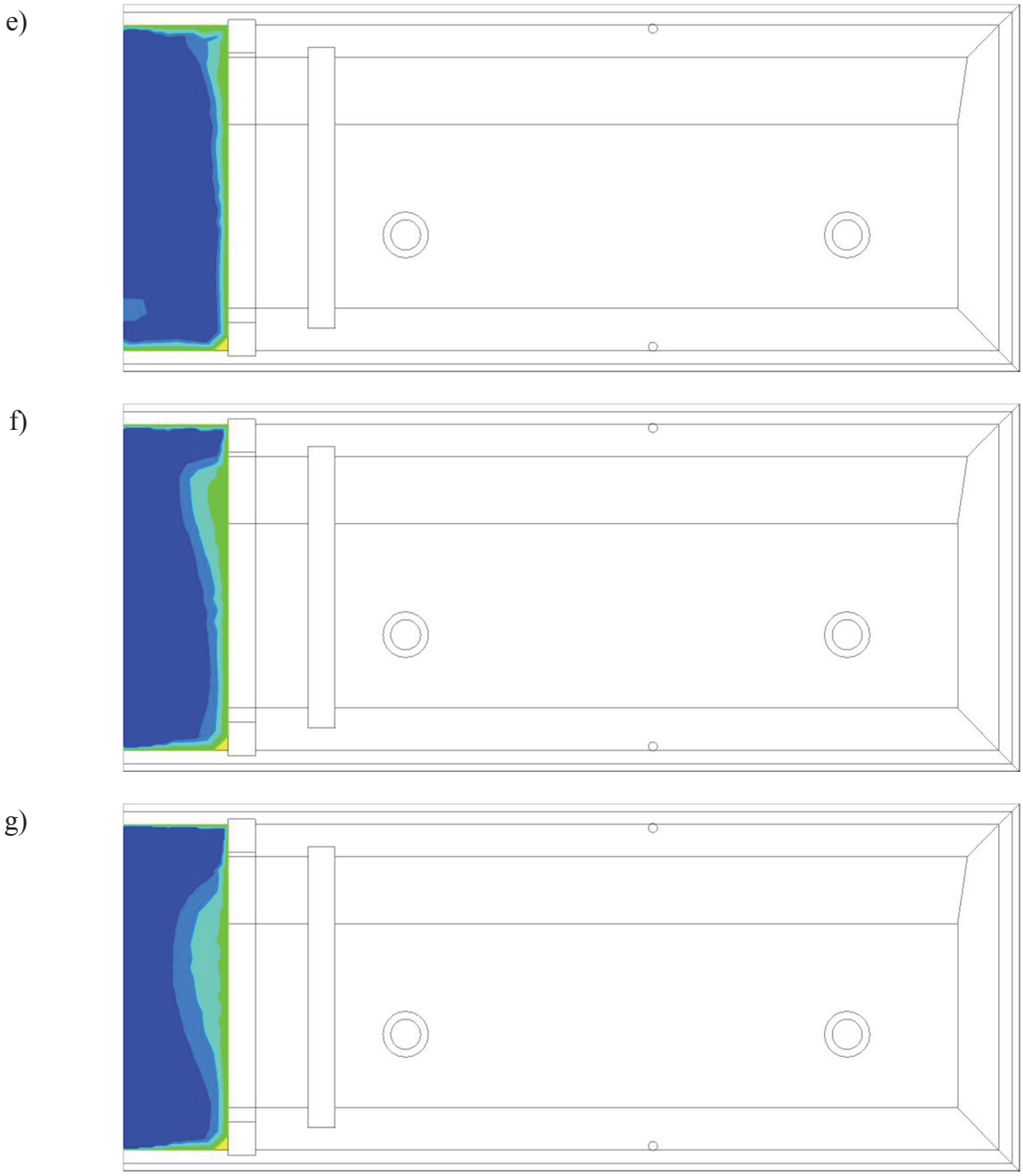

Fig. 4. *Contour plots for the normal velocity component at the lid opening at the end of purging. Negative values indicate air entry. Configurations of tundish inertization considering cold start: a) C1; b) C2; c) C3; d) C4; e) C5; f) C6;, g) C7.*

indicates about the risk of a common practice, the use the maximum gas flow rate available. Figure 5 shows the velocity profile of configuration C4 wherein air entry mechanism by turbulent jet entrainment is evident.

Perhaps the most obvious manner of avoiding air entry is to close or reduce lid openings, thus argon jet would be physically protected relative to atmospheric air. This idea was used in configuration C5. Air entry was almost eliminated (figure 4e) and purging efficiency was improved (N_{Ar} = 0.89) in relation to configuration C1 (N_{Ar} = 0.72). The beneficial effect of lid openings closure is enhanced in an indirect way. Since the lid openings area of configuration C5 (0.55m²) is only 32% of configuration C1 (1.70m²), the parameter J_{out} was nearly tripled.

Though jet protection troubleshoots the air entry problem of configuration C1, it may be interesting to use it together with configurations of injectors less likely to entrain air, as in C2 and C3, to make the process robust against a possible poor sealing of lid openings.

Configurations C6 (N_{Ar} = 0.97) and C7 (N_{Ar} = 0.99) show that, with proper control of air entry by physical protection of the argon jet (figure 4f and 4g, respectively), it is possible to improve purging effi-

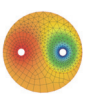

ciency by increasing gas flow rate. This is expected, since a greater flow rate promotes a faster renewal of the gas present within the tundish. While the flow rate of 105 Nm³/h (configuration C6) is sufficient to obtain residual oxygen content less than 1% (N_{air} < 0.05), the flow rate of 140 Nm³/h (configuration C7) is recommended because it allows to achieve the same result in a shorter time (3.2 min versus 4.3 min).

and considering cold start (figure 3). First, there are oscillations in the N_{Ar} curves of figure 6 that also appears in the T curves of figure 7. Such periodicity arises from the time variation of air entry into the tundish as can be observed in figure 8 and is related to the mechanism of natural convection. It is not a numerical problem, since all simulations converged and the oscillations persisted during studies of mesh and time-step independence. Secondly, N_{Ar}

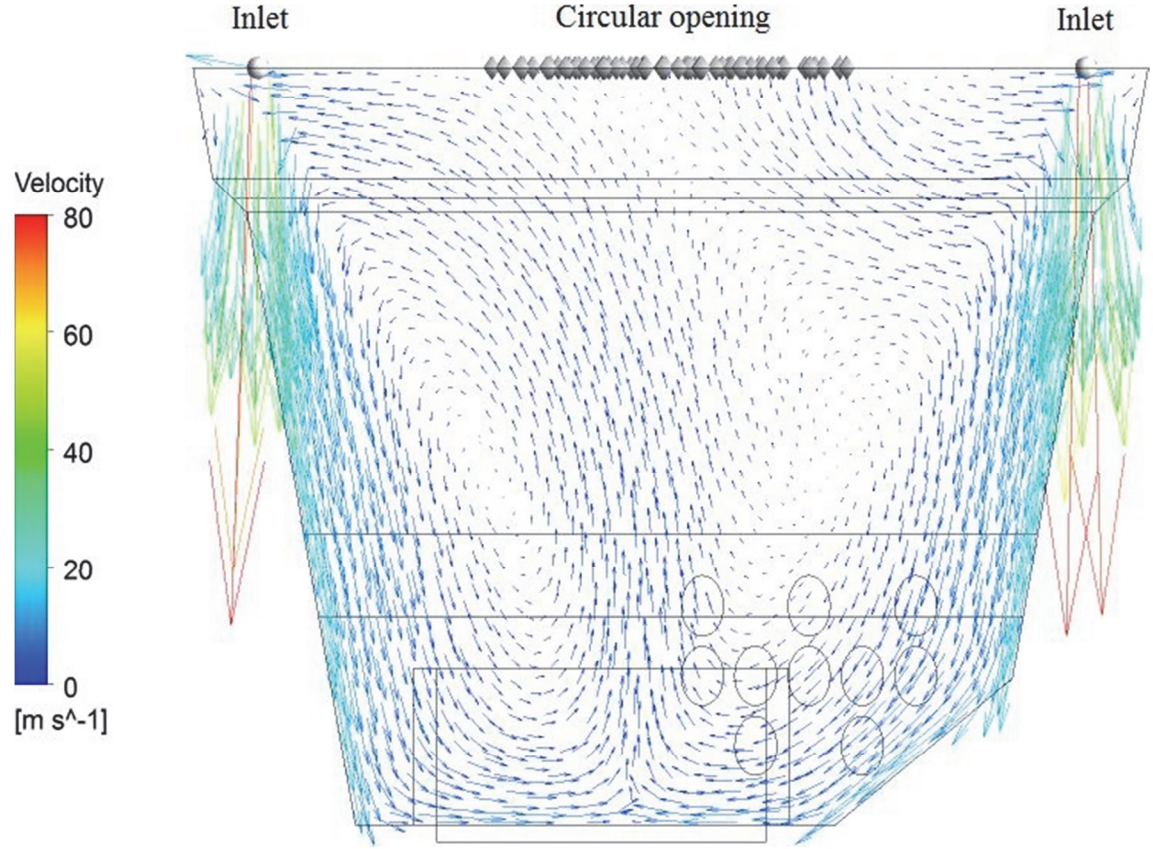

Fig. 5. *Velocity profile of configuration C4 at the end of purging plotted on a transverse plane cutting the injectors. The spheres indicate gas inlets and octahedrons point a lid opening.*

3.2. Inertization of Tundish Considering Hot Start

Figure 6 and 7 show the time variation of the average argon molar fraction (N_{Ar}) and average temperature (T), respectively, during purging for configurations of tundish inertization considering hot start. Table 7 summarizes N_{Ar} and T values at end of purging predicted by the mathematical model for the same configurations. Figure 8 shows contour plots for the normal velocity component at the lid opening at the end of purging for the previous configurations. Negative values indicate flow in inward direction and therefore point out air entry.

There are two main differences between inertization curves of tundish considering hot start (figure 6) curves stabilize more rapidly considering hot start than considering cold start. Indeed, the effective volumetric gas flow rate is enhanced in configurations of tundish considering hot start due to the significant expansion of the injected gas (figure 9).

Configuration H1, which is the actual practice used in the plant, has extremely low purging efficiency (N_{Ar} = 0.06) and much lesser than its cold version, configuration C1 (N_{Ar} = 0.72). The air entry is so severe (figure 10a) that the temperature of fluid inside the tundish was reduced to about 198ºC (figure 7). This is due to additional air entry by streams of natural convection that brings cold air through lid openings.

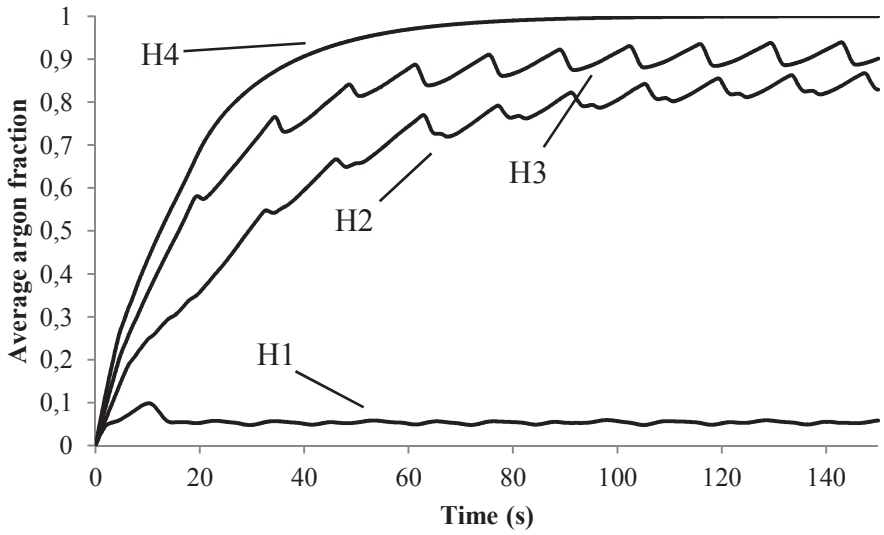

Fig. 6. *Time variation of average argon molar fraction (N_{Ar}) during purging for configurations of tundish inertization considering hot start. Values represent volumetric averages within the tundish.*

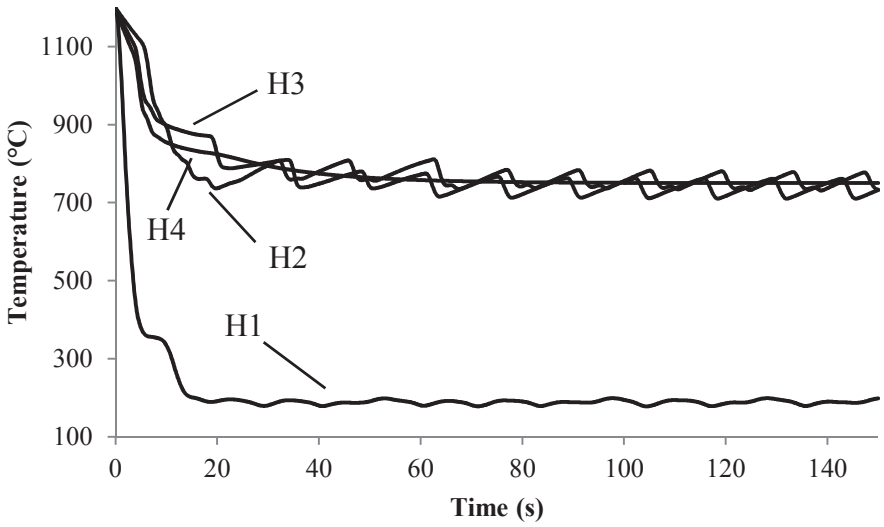

Fig. 7. *Time variation of average temperature (T) during purging for configurations of tundish inertization considering hot start. Values represent volumetric averages within the tundish.*

Table 7. *Average argon molar fraction (N_{Ar}) and average temperature (T) inside the tundish at the end of purging predicted by the mathematical model for configurations of tundish inertization considering hot start.*

Configuration	T (ºC)	N_{Ar}
H1	198	0.06
H2	733	0.83
H3	732	0.90
H4	750	1.00

Configuration H2 shows that lid openings closure is capable of reducing air entry (figure 10b) and substantially increasing purging efficiency (N_{Ar} = 0.83) compared to configuration H1. This improvement is due to simultaneous actions against the two driving forces for fluid flow, since J_{out} is increased by lid openings closure. The temperature of the fluid inside the tundish (approximately 733ºC) is also higher than in previous configuration which increases J_{out} even further.

Configuration H3 (N_{Ar} = 0.90) shows that purging efficiency of configuration H2 may be improved by increasing argon flow rate (70Nm³/h to 105Nm³/h). However, the reason is different from configurations considering cold start. For tundish with hot start, the time required to stabilize N_{Ar} curves is not affected by argon flow rate, as can be seen comparing configurations H2 and H3 in figure 6. Air entrainment of configuration H3 is reduced,

but it is not completely eliminated. Figure 10c is misleading due to the periodicity of air entry. The decrease of air entrainment is expected, since parameter J_{out} is augmented with increase of the argon flow rate.

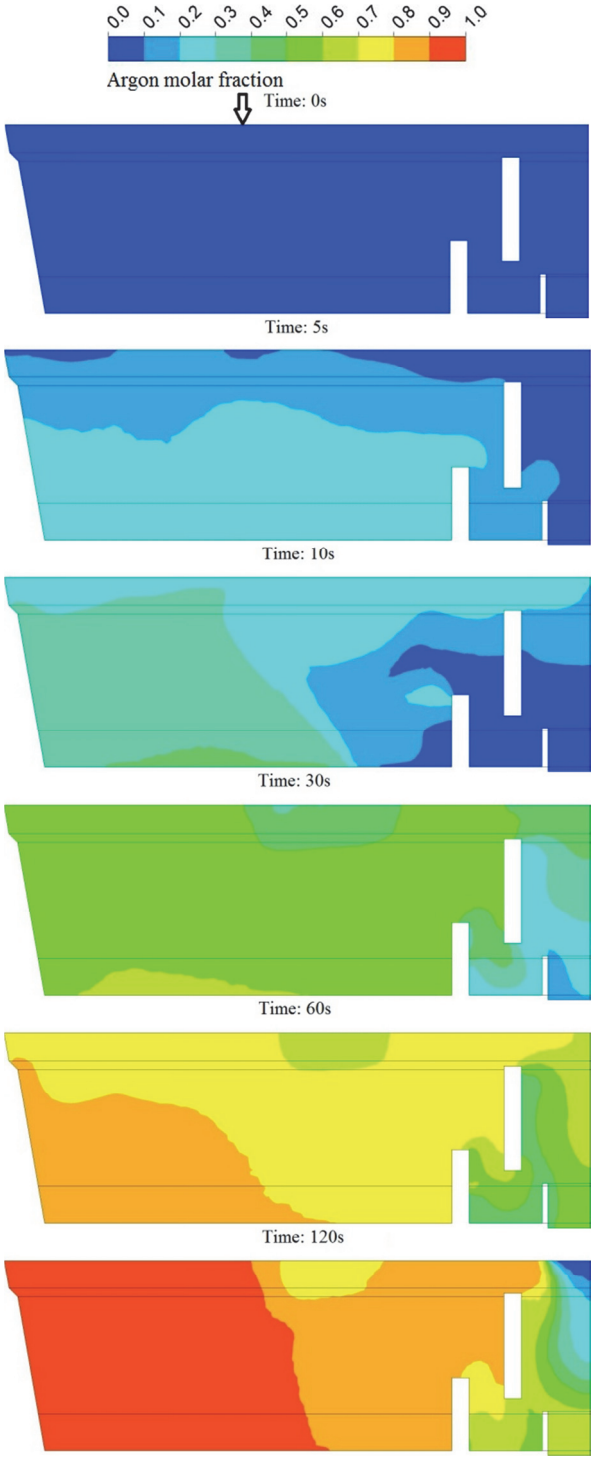

Fig. 8. *Contours of argon molar fraction predicted by the mathematical model for the configuration H2. The contours were created on the central plane of the tundish. The arrow on first figure indicates the point of argon injection.*

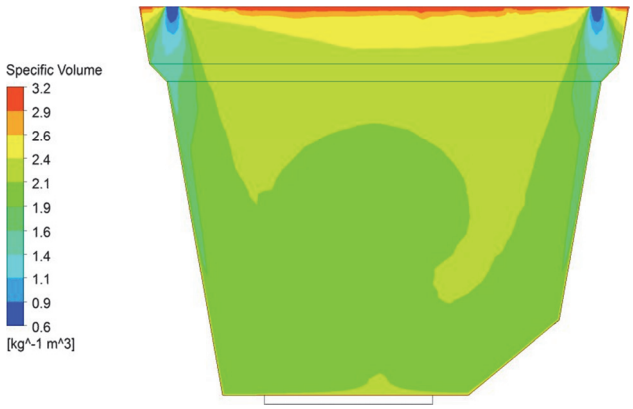

Fig. 9. *Specific volume (reciprocal of density) contour of configuration H2 at end of purging. The contour was created on a transverse plane cutting the injectors.*

Increase of the argon flow rate to 140Nm³/h (configuration H4) prevents air entrainment (figure 10d) and completely inertize the tundish (N_{Ar} = 1.00). Interestingly, purging efficiency of configuration H4 (N_{Ar} = 1.00) is higher than its cold version, configuration C7 (N_{Ar} = 0.99). This result is explained by the argon expansion that occurs in tundish with hot start as has already been discussed. Such phenomena is only noticed in absence of air entrainment.

It is noteworthy that fluid temperature of configurations H2 to H4 (figure 7 and table 7) was not significantly affected by the argon flow rate, although this gas is injected at 25ºC in the tundish. As a consequence, driving force for fluid flow R_b, a function of temperature, is not affected and heat loss from refractories, used to heating the injected gas, is enhanced almost linearly with argon flow rate.

4. CONCLUSIONS

A mathematical model was developed and used to investigate different configurations for tundish inertization system of a Brazilian steel plant. The system of partial differential equations involved was solved using ANSYS CFX. It was concluded that:

- For the tundish in study, the recommended inertization practice for both cold start and hot start is argon flow rate of 140Nm³/h and lid openings closure;
- It is also interesting to increase number (4 to 12) or diameter (25.4mm to 76.2 mm) of injectors to make the inertization process robust against a possible poor sealing of lid openings;
- Increased argon flow rate may lead to lower purging efficiency, if air entry is not prevented.

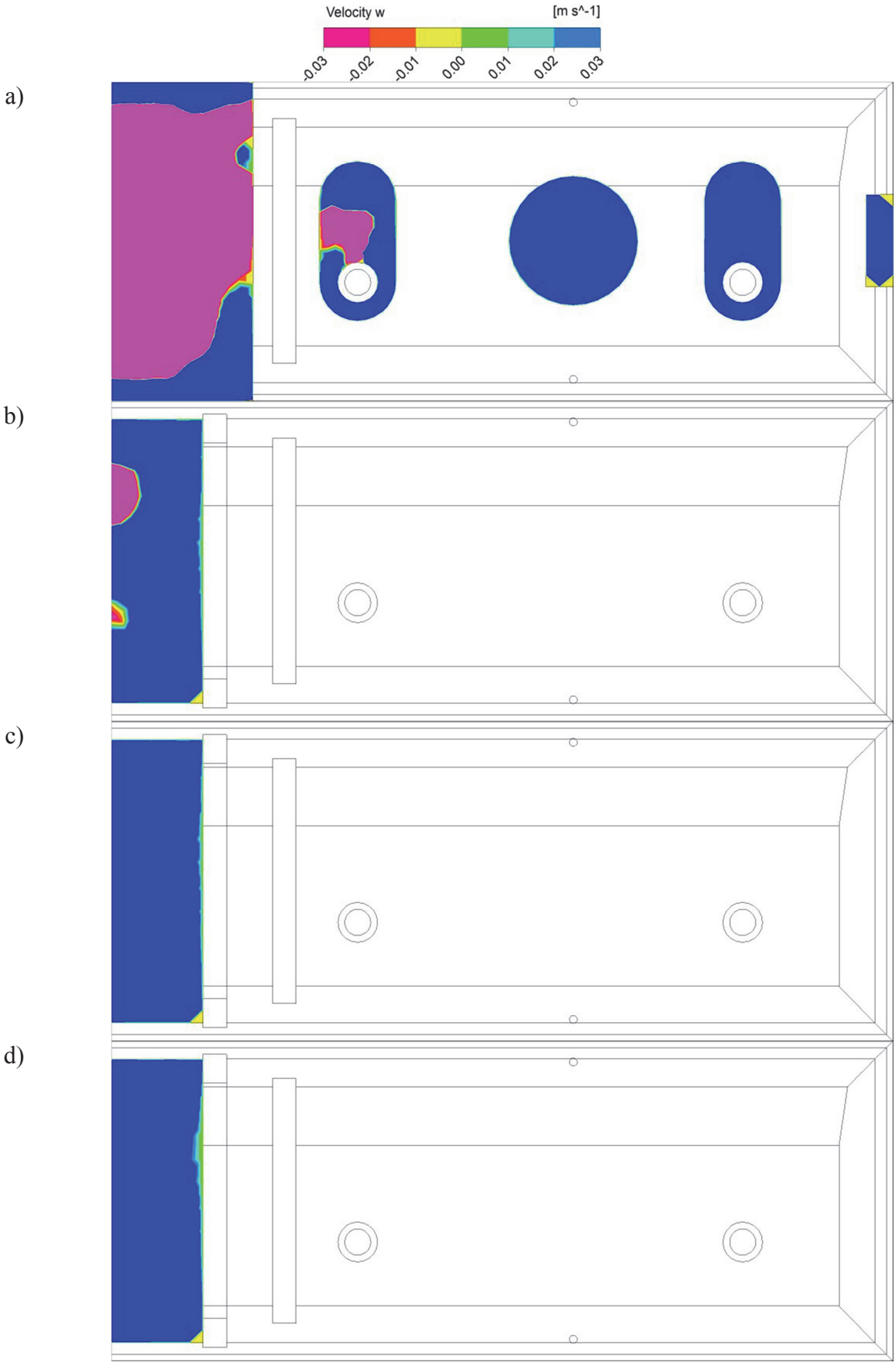

Fig. 10. *Contour plots for the normal velocity component at the lid opening at the end of purging. Negative values indicate air entry. Configurations of tundish inertization considering hot start: a) H1; b) H2; c) H3; d) H4.*

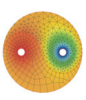

ACKNOWLEDGEMENTS

The financial support of FAPEMIG – Fundação de Amparo à Pesquisa do Estado de Minas Gerais, Brazil - in the form of a research grant to R. Tavares, Process No. PPM-00118-13, is gratefully acknowledged.

The authors also acknowledge the financial support of CAPES/PROEX to the graduate program.

The scholarship from CNPq to the first author is also gratefully acknowledged.

REFERENCES

Ansys, 2012, *ANSYS CFX-Solver Theory Guide*, Canonsburg.

Atkins, P., De Paula, J., 2006, *Atkins' Physical Chemistry*, eds, Crowe, J., Fiorillo, J., Hughes, R., Oxford University Press, New York.

Bannenberg, N., Harste, K., 1993, Improvements in Steel Cleanliness by Tundish Inertisation, *La Revue de Métallurgie*, 90, 71-76.

Bich, E., Millat, J., Vogel, E., 1990, The Viscosity and Thermal Conductivity of Pure Monatomic Gases from their Normal Boiling Point up to 5000 K in the limit of zero density and at 0.101325 MPa, *Journal of Physical and Chemical Reference Data*, 19, 1289-1305.

Bird, R.B., Stewart, W.E., Lightfoot, E.N., 2002, *Transport Phenomena*, John Wiley & Sons, New York.

Bonilla, C., 1995, Slivers in Continuous Casting, *Proc. Conf. Steelmaking '95*, 743-752.

Buoro, S., Romanelli, G., 2012, Technological Review of the Start-Up of a New Jumbo Bloom Continuous Caster for Specialty Steels, *Iron & Steel Technology*, 9, 39-47.

Chen, J.-H., Chen, C.-C., Yang, C.-Y., Yang, C.-C., 2005, Development of Inert Casting System for Slab Caster in CSC, *Proc. Conf. AISTECH '05*, 635-642.

Hughes, K.P., Schade, C.T., Shepherd, M.A., Weyant, J.W., 1995, Improvement in the Internal Quality of Continuously Cast Slabs at Lukens Steel, *Iron & Steelmaker*, 22, 35-41.

Incropera, F.P., DeWitt, D.P., Bergman, T.L., Lavine, A.S., 2006, *Fundamentals of Heat and Mass Transfer*, Willey, Hoboken.

Mattedi, S., Furtado, H.S., Garcia, U.M., Guimarães F.M.Q., Barbabela B.A., Rubião, L.E.G., 2003, Argon Injection Optimization at the CST Continuous Casting Machine, *Proc. Conf. AISE Annual Convention and Exposition '03*, Association of Iron and Steel Engineers, 1-22.

Riley, M.F., 1996, Control of Gas Turbulence in Purging of Caster Tundishes, *Proc. Conf. Steelmaking '96*, Iron and Steel Society, 513-518.

Uesugi, T., 1985, Production of High Carbon Chromium Bearing Steel by Vertical Type Continuous Caster, *Tetsu-to-Hagané*, 71, 1631-1638.

Yuan, C., 2009, Reduction of Blister Defects in Steel Plates, *SEAISI Quarterly Journal*, 38, 16-19.

Zhang, L., Thomas, B.G., 2003, State of the Art in Evaluation and Control of Steel Cleanliness, *ISIJ International*, 43, 271-291.

MATEMATYCZNE MODELOWANIE PROCESU TWORZENIA ATMOSFERY OBOJĘTNEJ W PRZESTRZENI ROBOCZEJ KADZI POŚREDNIEJ

Streszczenie

W pracy omówiono modelowanie procesu wytwarzania atmosfery obojętnej w przestrzeni roboczej kadzi pośredniej ciągłego odlewania stali. Zastosowano przestrzenny model dla warunków zmiennej temperatury. Model uwzględnia fazę gazową składającą się z argonu i powietrza. Turbulencje w przepływie gazu modelowano za pomocą standardowej metody k-ε. Symulacje CFD przepływu (ang. Computational Fluid Dynamics) wykonano w komercyjnym oprogramowaniu ANSYS CFX. Rozważono różne konfiguracje procesu tworzenia atmosfery obojętnej. Analiza wyników symulacji wykazała, że obecnie stosowana konfiguracja procesu jest nieefektywna. Na podstawie przeprowadzonej analizy uzyskanych wyników zaproponowano nowe podejście do tego procesu.

Received: August 15, 2014
Received in a revised form: September 3, 2014
Accepted: September 24, 2014